STATISTICAL MODELS OF NONEQUILIBRIUM BOSE GASES

V. I. YUKALOV[1,*], E. P. YUKALOVA[2]

[1]Bogoliubov Laboratory of Theoretical Physics,
Joint Institute for Nuclear Research, Dubna 141980, Russia
[2]Laboratory of Information Technologies,
Joint Institute for Nuclear Research, Dubna 141980, Russia
*Corresponding author *E-mail*: yukalov@theor.jinr.ru

Abstract. The idea is advanced that strong perturbations of an initially equilibrium Bose-condensed gas lead to the sequence of nonequilibrium states whose order is inverse to the sequence of states arising in the process of the Bose-gas relaxation from an initial nonequilibrium state. An approach is described for constructing statistical models of nonequilibrium Bose gases. The method is based on the averaging over heterogenous configurations of a nonequilibrium system. A statistical model of grain turbulence is suggested. A simple model is analyzed consisting of a mixture of two phases, one gauge symmetric and the other with broken gauge symmetry.

1. INTRODUCTION

The description of nonequilibrium systems is notoriously difficult, since such systems are usually strongly nonuniform and their dynamical states may quickly vary. However, when it is possible to separate in the system dynamics a regime exhibiting specific properties during sufficiently long time, longer that the time of fast local oscillations, then it may be admissible to average over the local fluctuations and to reduce the consideration to an effective quasi-stationary system, whose treatment is essentially simpler than that of the generic nonequilibrium system. As examples, we can mention the statistical models of fully developed vortex turbulence [1-3], heterophase models of quasi-equilibrium systems [4,5], and effective averaged models of nonequilibrium trapped atoms subject to periodic perturbations [6].

In the present paper, we describe a general approach for constructing effective quasi-stationary models for nonequilibrium systems. The approach is applicable when a nonequilibrium system exhibits some specific properties during sufficiently long time that is longer than the characteristic time of fast oscillations.

The transfer of a system from an equilibrium state to nonequilibrium states can be done by imposing external perturbations. For example, a system can be subject to a time-dependent perturbation potential $\hat{V}(t)$. Then the energy injected into the

system by this potential is defined as

$$E_{inj} \equiv \int_0^t \left| \left\langle \frac{\partial \hat{V}(t')}{\partial t'} \right\rangle \right| dt'.$$

In an averaged statistical picture, the injected energy acts similarly to temperature in equilibrium systems. Therefore, for a nonequilibrium system of N atoms, it is possible to introduce the effective temperature

$$T_{eff} \equiv \frac{E_{inj}}{k_B N},$$

which, for brevity, we may denote just as T.

The outline of the paper is as follows. In Sec. 2, a typical way of creating strongly nonequilibrium Bose-condensed gases is described and the characteristic parameters of Bose-condensed gases, used for creating such strongly nonequilibrium states, are discussed in order to give the feeling of the scales involved in experiments with nonequilibrium trapped atoms. In Sec. 3, we advance the idea that the procedure of generating a strongly nonequilibrium Bose system from an initially equilibrium Bose-Einstein condensate follows the same sequence of states, although in the reverse order, as the process of relaxation of an initially strongly nonequilibrium Bose system equilibrating to its condensed state. In Sec. 4, we describe the general method of deriving effective quasi-stationary models for nonequilibrium systems. The method is based on averaging over heterogeneous configurations arising in the treated nonequilibrium system. The consideration is exemplified in Sec. 5 by a statistical model of grain turbulence. In Sec. 6, we study a simple statistical model representing a nonequilibrium mixture of two phases with different symmetries, one gauge symmetric and the other with broken gauge symmetry. Section 7 gathers our concluding remarks.

When it does not lead to confusion, we employ the system of units where the Planck and Boltzmann constants are set to unity.

2. EXCITATION OF TRAPPED BOSE-EINSTEIN CONDENSATES

Trapped atoms provide a convenient tool for studying strongly nonequilibrium states of quantum systems. In the process of excitation, an atomic system passes through a sequence of qualitatively different states. The system of trapped condensed atoms can be strongly perturbed by an external field, when gradually increasing its strength and time of action.

Trapped Bose atoms in equilibrium at low temperatures form Bose-Einstein condensate in the ground state. The condensate cloud in a trap enjoys approximately Thomas-Fermi shape, with well known properties described in the books [7-9] and

reviews [10-19]. In order to break the condensate into pieces, it is necessary to impose external perturbations transferring the condensate from its ground state to excited states. There are two main ways of imposing such external perturbations.

One possibility is to add to the static trapping potential $U(\mathbf{r})$ an alternating potential $V(\mathbf{r},t)$, so that the total trap potential becomes

$$U(\mathbf{r},t) = U(\mathbf{r}) + V(\mathbf{r},t). \tag{1}$$

Another way is to modulate the scattering length $a_s(t)$ by means of Feshbach resonance techniques. Both these ways can be used for strongly perturbed condensates [19].

Suppose trapped Bose atoms have been cooled down to very low temperatures, when practically all of them pile down to a Bose-condensed state. And let us apply an external modulating perturbation by one of the methods mentioned above. First, at weak perturbations, there appear elementary collective excitations, that are small deviations from the ground state. Weak perturbations also can generate large deviations from the ground state, provided that the modulation frequency is in resonance with one of the transition frequencies between *topological coherent modes* [20]. The latter are defined as the eigenfunctions of the stationary nonlinear Schrödinger (NLS) equation

$$\left[-\frac{\nabla^2}{2m} + U(\mathbf{r}) + N\Phi_0 |\varphi_n(\mathbf{r})|^2 \right] \varphi_n(\mathbf{r}) = E_n \varphi_n(\mathbf{r}), \tag{2}$$

where N is the number of condensed atoms, assumed to be close to the total number of atoms, and

$$\Phi_0 \equiv 4\pi \, \frac{a_s}{m} \tag{3}$$

is the atomic interaction strength, in which a_s is a scattering length assumed to be positive. The modes are termed topological, since different modes have different numbers of zeroes, thus, topologically different atomic densities. The modes are coherent, being formed by condensed atoms characterized by coherent states.

The known particular example of the topological modes are quantum vortices. If the external perturbation rotates the atomic cloud, acting as a spoon, then vortices appear being aligned along the imposed axis of rotation. But when the trap modulation does not prescribe a fixed rotation axis, then vortices and antivortices arise in pairs or in larger groups [10,20]. The explicit experimental demonstration for the appearance of clusters of vortices and antivortices was done in Ref. [21].

Increasing the strength of the trap modulation generates a variety of coherent modes, needing no resonance conditions because of the power broadening effect [22]. Among these numerous coherent modes, the basic vortex, with the winding number one, is the most energetically stable. For a trap with a transverse, $\omega_\perp$, and

longitudinal, ω_z, frequencies, the vortex energy can be written [9] as

$$\omega_{vor} = \frac{0.9\omega_\perp}{(\nu g)^{2/5}} \ln(0.8\nu g), \qquad (4)$$

where the notation is used for the trap aspect ratio

$$\nu \equiv \frac{\omega_z}{\omega_\perp} = \left(\frac{l_\perp}{l_z}\right)^2 \qquad (5)$$

and for the effective coupling parameter

$$g \equiv 4\pi N \frac{a_s}{l_\perp}, \qquad (6)$$

with $l_\perp$ and l_z being the transverse and longitudinal oscillator lengths, respectively. Due to the large number of atoms N, the effective coupling parameter is large, $g \gg 1$. As is seen, the basic vortex energy diminishes with the increase of g. At the same time, the transition frequencies of other modes, hence their energies, can be shown [20,22] to increase as

$$\omega_{mn} \propto (\nu g)^{2/5} \qquad (g \gg 1). \qquad (7)$$

This makes the basic vortex the most energetically stable mode.

When the trap aspect ratio is not too small, the trap can house many vortices, whose number can be estimated as

$$N_{vor} \sim \frac{E_{inj}}{\omega_{vor}}, \qquad (8)$$

where E_{inj} is the energy injected into the trap by the external pumping. The vortices are created due to dynamical instability arising in the moving fluid [23-30].

Increasing the strength of the pumping, without imposing a rotation axis, produces a tangle of vortices, which makes the trapped atomic cloud turbulent [31-34]. Increasing further either the amplitude of the pumping field or the pumping time leads to the appearance of the condensate granulation [35].

The energy per particle, injected into the trap by the external perturbation, as is explained in the Introduction, plays the role of an effective temperature

$$T_{eff} = \frac{1}{N} \int \rho(\mathbf{r},t) \left| \frac{\partial V(\mathbf{r},t)}{\partial t} \right| d\mathbf{r}dt, \qquad (9)$$

where $\rho(\mathbf{r},t)$ is atomic density. In the case of the periodic in time alternating field $V(\mathbf{r},t) \sim A\cos(\omega t)$, the energy per atom, injected during the time interval $[t_1, t_2]$, takes the form $T_{eff} \approx \omega(t_1 - t_2)$. This makes it possible to represent the crossover lines between different regimes as the relation

$$A = \frac{T_{eff}}{\omega(t_1 - t_2)} \qquad (10)$$

between the amplitude A of the pumping field and the pumping time.

The experimental phase diagram on the amplitude-time $A - t$ plane is described in Refs. [33-35], where it is shown that with increasing the injected energy, that is proportional to the product At, the system passes through the following states: *regular superfluid* slightly perturbed by a weak external field, *vortex superfluid* with several vortices, *turbulent superfluid* formed by a tangle of many vortices, and *granular state* with condensate droplets surrounded by uncondensed gas.

To give the reader the feeling of the typical parameters in the experiments with trapped atomic gases, let us mention the corresponding characteristic quantities and experimental data.

The size of an atomic cloud can be found by solving the nonlinear Shrödinger (NLS) equation and calculating the mean-square lengths in the corresponding directions. For a cylindrical trap, taking into account that $g \gg 1$, this gives [10,20,22] the mean transverse radius

$$r_\perp = \frac{(2\nu g)^{1/5} l_\perp}{(2\pi)^{3/10}} = 0.662 (\nu g)^{1/5} l_\perp \tag{11}$$

and the mean axial radius

$$z_0 = \frac{(\nu g)^{1/5} l_z}{(4\pi)^{3/10} \sqrt{\nu}} = 0.468 \frac{(\nu g)^{1/5}}{\sqrt{\nu}} l_z, \tag{12}$$

where the standard notations are used for the effective transverse oscillator length $l_\perp \equiv \sqrt{\hbar/m\omega_\perp}$ and longitudinal oscillator length $l_z \equiv \sqrt{\hbar/m\omega_z}$, and where ν is the trap aspect ratio. The mean effective cloud radius is

$$r_0 \equiv \left(r_\perp^2 z_0\right)^{1/3} = 0.59 \frac{(\nu g)^{1/5}}{\nu^{1/6}} l_0, \tag{13}$$

where the average oscillator length is

$$l_0 \equiv \sqrt{\frac{\hbar}{m\omega_0}}, \qquad \omega_0 = \left(\omega_\perp^2 \omega_z\right)^{1/3}.$$

As we see, the actual cloud sizes are noticeably larger than the oscillator lengths because of repulsive atomic interactions. These sizes even can be essentially larger than the oscillator lengths, when $g \gg 1$.

Knowing the size of the trapped atomic cloud, it is straightforward to find the effective cloud volume

$$V_{eff} \equiv \pi r_\perp^2 2 z_0 = 2\pi r_0^3 = 1.29 \frac{(\nu g)^{3/5}}{\sqrt{\nu}} l_0^3 \tag{14}$$

and to estimate the average atomic density in the trap

$$\rho \equiv \frac{N}{V_{eff}} = 0.775 \frac{\sqrt{\nu} N}{(\nu g)^{3/5} l_0^3}. \tag{15}$$

This shows that, for strongly repulsive atoms, the atomic density ρ can be much smaller than the density N/l_0^3 they would have in the absence of repulsive interactions.

Pair atomic interactions are conveniently characterized by the gas parameter

$$\gamma \equiv \rho^{1/3} a_s = \frac{a_s}{a}, \tag{16}$$

where $a = \rho^{1/3}$ is mean interatomic distance. The gas parameter γ is usually small for trapped atoms, though can be varied in a wide range by means of the Feshbach resonance techniques. Because of the large number of atoms in a trap, the effective coupling parameter g is usually large.

An important quantity, showing whether atoms are in local equilibrium, is the local equilibration time $t_{loc} \sim m/\hbar\rho a_s$. A perturbed cloud of trapped atoms can, as a whole, be strongly nonequilibrium, while, at the same time, be locally equilibrium. This happens in the situation, when the modulation period $t_{mod} \equiv 2\pi/\omega$ of the alternating modulating field, with frequency ω, is much longer than the local equilibration time t_{loc}.

In experiments [33-35], strongly nonequilibrium states were generated by modulating the trapping potential for a trapped cloud of ^{87}Rb. The cloud of ^{87}Rb atoms, of mass $m = 1.443 \times 10^{-22}$ g and scattering length $a_s = 0.557 \times 10^{-6}$ cm, has been cooled down to the temperatures much lower than the Bose-Einstein condensation temperature $T_c = 276$ nK, so that the great majority of all $N = 2 \times 10^5$ atoms have been condensed, the condensate fraction being $n_0 = 0.7$.

The trap had cylindrical shape, with the parameters

$$\omega_\perp = 1.32 \times 10^3 \text{s}^{-1}, \qquad \omega_z = 1.45 \times 10^2 \text{s}^{-1},$$

$$l_\perp = 0.74 \times 10^{-4} \text{cm}, \qquad l_z = 2.25 \times 10^{-4} \text{cm},$$

$$\omega_0 = 0.63 \times 10^3 \text{s}^{-1}, \qquad l_0 = 1.08 \times 10^{-4} \text{cm}, \tag{17}$$

which gives the trap aspect ratio $\nu = 0.11$. The effective coupling parameter is $g = 1.96 \times 10^4$.

The atomic cloud is characterized by the sizes

$$r_\perp = 2.27 \times 10^{-4} \text{cm}, \qquad z_0 = 1.47 \times 10^{-3} \text{cm},$$

$$r_0 = 0.42 \times 10^{-3} \text{cm}, \qquad V_{eff} = 0.47 \times 10^{-9} \text{cm}^3, \tag{18}$$

which define the effective atomic density $\rho = 0.43 \times 10^{15}$ cm^{-3} and the mean interatomic distance $a = 1.32 \times 10^{-5}$ cm. The gas parameter is $\gamma = 0.044$.

The trap potential was modulated by an additional alternating potential $V(\mathbf{r}, t)$ [36,37] oscillating with frequency $\omega = 1.26 \times 10^3$ s^{-1}, which corresponds to the

modulation period $t_{mod} = 0.5 \times 10^{-2}$ s. The total modulation time t_{ext} was varied between 0.02 s and 0.1 s. The local equilibration time is $t_{loc} = 0.57 \times 10^{-3}$ s. Thus, the relations between the characteristic times is $t_{loc} \ll t_{mod} \ll t_{ext}$.

Because of the high atomic density inside the trap, the *in situ* observation was impossible. Absorption pictures were taken in the time-of-flight setup, after the times t_{tof} between 0.015 s and 0.023 s. Restoring the characteristic linear size of granules, corresponding to the experimental situation before the free expansion, one gets [35] $l_g \approx 3 \times 10^{-5}$ cm. This is in agreement with the theoretical evaluation of the grain size assumed to be of the order of the coherence length $\xi = 1/\sqrt{4\pi\rho a_s}$. Thus, the relation between the characteristic lengths is $a_s \ll a \sim \xi \sim l_g \ll l_0 < r_0$.

The excitation of strongly nonuniform states can also be realized by modulating the scattering length [38,39]. Generally, long modulation times or large exciting amplitudes generate the cloud evolution from the appearance of separate vortices to tangled vortex configurations, typical of quantum turbulence, and to the granular state.

To compare the parameters in the experiments with trapped ^{87}Rb atoms with the typical parameters of other experiments with trapped atoms, let us consider the case of ^{7}Li in a light trap formed by focused laser beams, as described in Refs. [40,41]. The atoms of ^{7}Li of mass $m = 1.2 \times 10^{-23}$ g are prepared, using Feshbach resonance techniques [42], at the scattering length $a_s = 3.2 \times 10^{-8}$ cm. Lowering down temperature, essentially below the critical condensation temperature $T_c = 200$ nK, almost all $N = 3 \times 10^5$ trapped atoms are Bose-condensed, with the condensate fraction $n_0 = 0.9$.

The trap characteristics are

$$\omega_\perp = 1.48 \times 10^3 \text{s}^{-1}, \qquad \omega_z = 30.4 \text{s}^{-1},$$

$$l_\perp = 2.5 \times 10^{-4} \text{cm}, \qquad l_z = 1.7 \times 10^{-3} \text{cm},$$

$$\omega_0 = 4.1 \times 10^2 \text{s}^{-1}, \qquad l_0 = 4.7 \times 10^{-4} \text{cm}, \tag{19}$$

which give the trap aspect ratio $\nu = 0.0207$. This means that the trap is quasi-one-dimensional.

The cloud shape corresponds to the sizes

$$r_\perp = 2.62 \times 10^{-4} \text{cm}, \qquad z_0 = 0.88 \times 10^{-2} \text{cm},$$

$$r_0 = 0.84 \times 10^{-3} \text{cm}, \qquad V_{eff} = 0.38 \times 10^{-8} \text{cm}^3, \tag{20}$$

which define the effective density $\rho = 0.79 \times 10^{14}$ cm^{-3} and the mean interatomic distance $a = 2.33 \times 10^{-5}$ cm. This density is an order lower than that for ^{87}Rb. The lower density and the larger spatial size allows to observe the behavior of the

atomic cloud *in situ*. The gas parameter is $\gamma = 1.37 \times 10^{-3}$. The effective coupling parameter is $g = 0.48 \times 10^3$.

The effective scattering length

$$a_s(t) = a_{BG}\left[1 - \frac{\Delta B}{B(t) - B_\infty}\right]$$

can be modulated by varying the magnetic field

$$B(t) = B_0 + \delta B \cdot \cos(\omega t).$$

Here a_{BG} is a background scattering length far from the resonance field B_∞, and ΔB is the resonance width.

In the case, when δB is much smaller than B_0, one can write the oscillating scattering length in the form

$$a_s(t) \cong a_s + \delta a_s \cdot \cos(\omega t),$$

in which

$$a_s \equiv a_{BG}\left(1 - \frac{\Delta B}{B_0 - B_\infty}\right), \qquad \delta a_s \equiv a_{BG}\frac{\Delta B \delta B}{(B_0 - B_\infty)^2}.$$

The amplitude of the scattering-length oscillations corresponds to $\delta a_s/a_s = 0.2$. The frequency ω is varied in the range between 157 s^{-1} and 314 s^{-1}, which gives the modulation period t_{mod} between 2×10^{-2} s and 4×10^{-2} s. The local equilibration time $t_{loc} = 4.5 \times 10^{-3}$ s is much shorter than the modulation time, $t_{loc} \ll t_{mod}$.

At the beginning, the scattering-length modulation, generates quadrupole mode excitations. The amplitude of the oscillations as a function of the applied frequency, allows one to locate the resonance curve for the quadrupole mode excitations, as has been shown in Ref. [39].

The relation between the characteristic lengths, including the scattering length a_s, mean interatomic distance a, longitudinal oscillator length l_z, and the axial radius of the cloud z_0, is such that $a_s \ll a \ll l_z < z_0$.

The phase diagram on the amplitude-time $A - t$ plane, observed in the experiments with a strongly perturbed gas of ^{87}Rb, is discussed in Refs. [33-35]. And the detailed results for a strongly nonequilibrium gas of ^{7}Li will be published in a separate paper.

3. NONEQUILIBRIUM CONDENSATION VERSUS STRONG PERTURBATION

In the process of strong perturbation, trapped Bose gases pass through several nonequilibrium states, such as the *vortex state* with a few vortices, strong *vortex turbulence*, and *granular state*. Increasing further perturbation should completely

destroy the condensate, transferring the whole system into a chaotic normal state with no condensate [35].

To our understanding, the sequence of dynamic states, appearing in the process of strong perturbation of trapped Bose gases, should correspond, although in the reverse order, to the sequence of dynamic states, arising in the process of equilibration of an initially strongly nonequilibrium Bose system to its equilibrium Bose-condensed state.

The equilibration of weakly interacting Bose systems, from an initial strongly nonequilibrium normal state to Bose-condensed state has been studied in a number of publications. Levich and Yakhot [43] tried to describe this process by a kinetic equation for the occupation number of particles. They found that the time of Bose condensation is infinite, and becomes finite only if the presence of germs of the Bose-condensed phase at the beginning of the cooling process is assumed. Thus, the single *kinetic stage* cannot result in Bose-Einstein condensation.

Stoof [44,45] employed a functional approach in the frame of the Keldysh formalism for deriving a time-dependent Ginzburg-Landau theory and a Fokker-Planck equation for the initial stages of nonequilibrium Bose-Einstein condensation. He distinguishes three stages of the nonequilibrium condensation. After the Bose gas is quenched into the critical region of the phase transition, at the first stage, it can be described by the quantum Boltzmann equation. However, such a kinetic equation cannot describe the buildup of coherence in the gas and therefore does not lead to a microscopic occupation of the single-particle state. In other words, incoherent collisions, governing the Boltzmann kinetic equation, cannot lead to Bose-Einstein condensation [43]. To achieve this, a second stage is needed, in which the gas develops the instability toward Bose condensation and then coherently populates the ground state by a depletion of the low-lying excited states. The assumed instability, developing in the coherent stage, is analogous to a dynamic phase transition. After the coherent stage, the gas acquires a highly nonequilibrium energy distribution, and equilibrates during the third and final stage. This last stage is again of kinetic nature and can be described by the appropriate quantum Boltzman equation for the Bogoliubov quasiparticles of the Bose-condensed gas. In that way, according to Stoof, there are three stages of nonequilibrium condensation: *kinetic stage*, *coherent stage*, and *relaxation stage* that also is of kinetic type.

The kinetic Boltzmann equation was solved numerically by Snoke and Wolfe [46] and by Semikoz and Tkachev [47]. In the latter paper, the authors acknowledge the existence of three stages, as in the Stoof picture, but treat only two kinetic stages. At the first stage, the condensate is absent, but there is a nonzero inflow of particles towards the zero momentum state. In the framework of the kinetic equation, there is no condensate at all times if there was no condensate initially. Therefore one has to add a seed condensate by hands when switching from the first kinetic stage to

the final kinetic stage. In this approach, the intermediate coherent stage, where the condensate actually emerges by a kind of a phase transition, is omitted.

The process of Bose condensation has also been considered by numerical solutions of the NLS equation assuming the presence of the solution random phase [48] or of external random noise [49]. The condensation stages were not clearly distinguished.

The occurrence of several stages in the nonequilibrium Bose condensation of a weakly interacting Bose gas has been emphasized by Kagan and Svistunov [50,51] and Berloff and Svistunov [52]. Strongly nonequilibrium Bose gas, after a very short time develops a highly chaotic state, where kinetic energy is much larger than the interaction energy. Because of the small nonlinearity, the system can be treated as a collection of almost independent modes with random phases. The smallness of correlations between the modes implies the absence of any order. This chaotic regime of normal (non-superfluid) gas is termed wave turbulence or weak turbulence. Assuming that the low-energy modes are macroscopically occupied (so that the occupation numbers are much greater than one), it is possible to represent the system by a coherent field with random phase. The modes propagate from relatively high to lower energies, and at some time the wave turbulence transforms into a regime where short-range coherence starts appearing. This is the regime of strong turbulence that cannot be characterized by quasi-independent modes. After this intermediate stage, the regime of superfluid turbulence arises, where numerous tangled vortices form a *random tangle*. This could also be called the vortex turbulence. The next stage is the process of relaxation of the vortex turbulence to an equilibrium state in a macroscopically long time. In this way, one can distinguish four stages: *wave turbulence*, *strong turbulence*, *vortex turbulence*, and *relaxation stage*. Since from the very beginning, one assumes that the low-energy modes are macroscopically occupied, the whole process becomes a crossover, with a continuous growth of the low-energy occupation numbers, the lowest of which represents Bose condensate. The intermediate regime of strong turbulence is equivalent, in the Stoof picture, to his coherent stage. The difference is that Stoof suggests that during this regime a kind of phase transition occurs, when the germs of Bose condensate suddenly appear. While in the Svistunov *et al.* picture, the low-energy modes are assumed to exist already in the regime of wave turbulence, just starting fast growing in the intermediate strong turbulence stage, so that there is not a phase transition but a sharp crossover. It has been mentioned [53] that the dynamics of the Bose-Einstein condensation is similar to the collapse dynamics of a self-gravitating gas.

The dynamics of the condensation of a weakly interacting Bose gas in a trap is analogous to that of the homogeneous gas [54] and can be characterized by a quantum kinetic equation, where the arising condensate comes from the bath of uncondensed atoms [55-57].

Zakharov and Nazarenko [58] distinguish four regimes in the dynamics of Bose-Einstein condensation. The first is the kinetic stage, when the system is forced into a nonequilibrium state corresponding to weak turbulence. The kinetic regime transfers into a strong-turbulence state, where the kinetic description breaks down. The second stage is the vortex turbulence, where there appear a number of vortices forming a chaotic tangle. In the third stage, the system is filled by a well developed condensate with just a few vortices. And the final stage corresponds to the relaxation to the equilibrium state. The authors [58] concentrated their attention on the strong-condensate regime containing a small number of vortices. They used the NLS equation complimented by a term describing forcing and dissipation.

The condensate dynamics from a nonequilibrium initial state have been studied experimentally [59-62], observing the simultaneous population growth and the development of the phase coherence. The regime of vortex turbulence was investigated in experiments [31-35,63] and reviewed in Refs. [35,64-67].

The regime of vortex turbulence, developing in the process of the nonequilibrium Bose-Einstein condensation, is the manifestation of the Kibble-Zurek mechanism [68-70] that has been observed [71] in the condensation of trapped ^{87}Rb atoms. In this picture [68-71], the vortex turbulence is preceded by the formation of a nonuniform structure composed of the coherent germs, called by Kibble [68] "cells", or "protodomains", of the condensed phase inside the cloud of uncondensed atoms. The order parameters of different cells are random, so that there is no coherence between different protodomains. Such domains move in space and can fuse with each other. According to Kibble [68], it is the cell fusion that creates vortices.

In order to clearly distinguish these nonequilibrium coherent cells, also called protodomains, from the static domains occurring in ferromagnets, we shall call these nonequilibrium germs the *grains*. Since their sizes are intermediate between the atomic interaction length and the system size, such mesoscopic germs of one phase inside another are analogous to the heterophase fluctuations [4,5]. These coherent grains appear for repulsive atomic interactions, and should not be confused with the bound droplet dew forming in a Bose gas with attractive interactions [72]. Because the shapes and spatial locations of the grains are random, the corresponding strongly nonequilibrium phenomenon can be termed *grain turbulence*. The regime of grain turbulence happens between the stages of wave turbulence and vortex turbulence, hence, corresponding to the stage of strong turbulence. This is the most difficult regime for theoretical description, being strongly nonequilibrium and produced by the chaotic motion of the grains of random shapes, which are randomly distributed in space.

To be more concrete, let us characterize the specific dynamic stages of nonequilibrium Bose systems. These stages are connected with the typical length and time scales of statistical systems [4,5,12]. For dilute gases, the shortest is the interaction

length r_{int} that is much smaller than the scattering length a_s. Other lengths are: the mean interatomic distance a, correlation length ξ, and the mean free path λ, for which we have

$$a \sim \frac{1}{\rho^{1/3}}, \qquad \xi \sim \frac{\hbar}{ms}, \qquad \lambda \sim \frac{1}{\rho a_s^2}, \qquad (21)$$

where ρ is the mean atomic density and

$$s \sim \frac{\hbar}{m}\sqrt{4\pi\rho a_s}$$

is sound velocity. For Bose gases, the typical relation between the lengths is

$$a_s < a < \xi < \lambda.$$

These lengths are connected with the characteristic velocities: the scattering velocity v_s, kinetic velocity v_a, and the sound velocity s, so that

$$v_s \sim \frac{\hbar}{ma_s}, \qquad v_a \sim \frac{\hbar}{ma}, \qquad s \sim \frac{\hbar}{m\xi}, \qquad (22)$$

with the typical relation

$$s < v_a < v_s.$$

The kinetic velocity shows the typical velocity of atoms between collisions, while the scattering velocity corresponds to the velocity of atoms in the process of their collisions.

The characteristic time scales, respectively, are as follows. The *interaction time*

$$t_{int} \sim \frac{a_s}{v_s} \sim \frac{ma_s^2}{\hbar} \qquad (23)$$

is the time of atomic interactions. The *local-equilibration time*

$$t_{loc} \sim \frac{\lambda}{v_s} \sim \frac{m}{\hbar\rho a_s} \qquad (24)$$

is the time during which there develops local equilibrium and there can arise correlated regions in space. The *heterophase time*

$$t_{het} \sim \frac{\xi}{a_s}t_{loc} \sim \frac{\lambda}{s} \sim \frac{1}{\rho a_s^2 s} \qquad (25)$$

is the lifetime during which there can exist well correlated regions in space, corresponding to protodomaion, or grains. The longer is the relaxation time t_{rel}, after which the system gradually relaxes to its equilibrium state during the equilibration time t_{equ}.

The intervals between the above times define the corresponding dynamic stages through which a Bose system passes, being initially prepared in a strongly nonequilibrium state by quickly quenching it to the conditions, where the Bose condensate

should occur. The first is the *interaction stage*, or *dynamic stage*,

$$0 < t < t_{int} \qquad (interaction \; stage),\tag{26}$$

during which atoms interact with each other a few times. At this short initial stage, statistical description is not yet applicable.

The second is the *kinetic stage*,

$$t_{int} < t < t_{loc} \qquad (kinetic \; stage),\tag{27}$$

where the system can be described by a kinetic equation. This stage corresponds to the regime of *wave turbulence*, or *weak turbulence*, when the kinetic energy is much larger than the interaction energy, so that the system can be represented as a collection of almost independent modes of small amplitudes. The mode independence is due to their spatial phases being random. Thus, the regime of wave turbulence is characterized by three features: *large kinetic energy*, *modes of small amplitude*, and *random spatial phases*. There is yet no condensate at this stage.

The third is the *heterophase stage*,

$$t_{loc} < t < t_{het} \qquad (heterophase \; stage),\tag{28}$$

when the kinetic description becomes not applicable, since atomic interactions and correlations start playing an important role, as a result of which the mode amplitudes grow, and there appear mesoscopic well correlated regions of locally condensed atoms. The regions are mesoscopic, having the typical sizes of the correlation length ξ that is between the scattering length a_s and the system size. This is the regime of *strong turbulence*, or *grain turbulence*. The atoms inside each grain are well correlated, forming a condensed droplet, but different grains are not necessarily correlated with each other and possess different random phases. The condensed grains are surrounded by a gas of normal uncondensed atoms.

The fourth is the *hydrodynamic stage*,

$$t_{het} < t < t_{rel} \qquad (hydrodynamic \; stage),\tag{29}$$

when the mesoscopic condensed grains fuse, forming quantum vortices, according to the Kibble-Zurek mechanism [68-71]. A tangle of numerous random vortices arises, creating the regime of quantum *vortex turbulence*. This regime can be described by superfluid kinetic equations [73] and superfluid hydrodynamic equations [74,75]. The hydrodynamic stage lasts till the relaxation time t_{rel} that depends on the system parameters and geometry [76,77].

After the relaxation time t_{rel}, the vortices decay by mutual recombination and phonon emission. For some time, a few vortices survive, but then the system tends to its equilibrium Bose-condensed state. This happens at the relaxation stage,

$$t_{rel} < t < t_{equ} \qquad (relaxation \; stage),\tag{30}$$

where t_{equ} is the equilibration time [76].

To illustrate the values of the characteristic parameters discussed above, let us consider the experiments [33-35] with trapped ^{87}Rb atoms. Then we have the scattering length $a_s = 0.557 \times 10^{-6}$ cm, mean interatomic distance $a = 1.32 \times 10^{-5}$ cm, correlation length $\xi \sim 1.823 \times 10^{-5}$ cm, mean free path $\lambda \sim 0.75 \times 10^{-2}$ cm, sound velocity $s \sim 0.401$ cm/s, kinetic velocity $v_a \sim 0.554$ cm/s, and the scattering velocity $v_s \sim 13.12$ cm/s. This defines the characteristic times: the interaction time $t_{int} \sim 4.245 \times 10^{-8}$ s, local-equilibration time $t_{loc} \sim 0.572 \times 10^{-3}$ s, and the heterophase time $t_{het} \sim 1.87 \times 10^{-2}$ s. The interaction time, as is expected, is very short, so that atoms quickly pass into the kinetic stage of wave turbulence which lasts around 10^{-3} s. The duration of the heterophase correlated stage is 1.8×10^{-2} s, after which the regime of vortex turbulence comes into play.

For other setups, the typical parameters can be rather different. For instance, in the case of ^{7}Li, as in experiments [40,41], we have the scattering length $a_s = 3.2 \times 10^{-8}$ cm, mean interatomic distance $a = 2.33 \times 10^{-5}$ cm, correlation length $\xi \sim 1.775 \times 10^{-4}$ cm, mean free path $\lambda \sim 12.36$ cm, sound velocity $s \sim 0.495$ cm/s, kinetic velocity $v_a \sim 3.772$ cm/s, and the scattering velocity $v_s \sim 2.746 \times 10^3$ cm/s. From here, we find the interaction time $t_{int} \sim 1.165 \times 10^{-11}$ s, local-equilibrium time $t_{loc} \sim 4.501 \times 10^{-3}$ s, and the heterophase time $t_{het} \sim 24.97$ s. The interaction time is again very short, and atoms quickly pass to the kinetic stage of the wave turbulence. But the heterophase correlated stage is quite long, of order of ten seconds. Hence, more time is needed for the development of the vortex turbulence, if any.

The above description corresponds to the relaxation of a Bose gas that initially is prepared in a strongly nonequilibrium normal state, after which it tends to its equilibrium condensed state. We suggest that when an initially equilibrium condensed Bose gas is subject to strong perturbations, it passes through the same dynamic stages, although in the reverse order, with the increasing amount of the energy pumped into the system. Thus, an initially condensed gas, being perturbed, first goes into a nonequilibrium state, where just a few vortices can arise. The next is the hydrodynamic stage, where the vortex turbulence develops. After this, the heterophase correlated stage should occur, where the grain turbulence takes place. Finally, when all condensate is destroyed, the regime of wave turbulence has to come. The sequence of these stages (except the last one) for a strongly perturbed Bose gas of ^{87}Rb atoms has been observed in experiments [33-35]. The total destruction of the condensate requires very strong perturbations that have not yet been reached in experiments.

The dynamic transitions between the different stages described above are, of course, not absolutely sharp, as would be phase transitions in equilibrium systems, but they are rather gradual crossovers.

4. AVERAGING OVER HETEROGENEOUS CONFIGURATIONS

Although the dynamic transitions between the nonequilibrium stages are cross-overs, inside the corresponding temporal intervals the system enjoys qualitatively well defined features. This means that it would be admissible to introduce quasi-stationary states as those of a system averaged over the appropriate time interval. This can be done as follows.

Let us assume that a nonequilibrium system can live quite long time, being supported by an external perturbation with an alternating modulation potential. If the local equilibration time is much shorter than the modulation period, then the system can be treated as quasi-equilibrium. The difficulty of theoretical description of such a system is in its nonuniformity, with randomly arising spatio-temporal fluctuations. When the external pumping potential does not impose a spatial symmetry, then the nonuniformities are randomly distributed at each snapshot and do not form any ordered structure. Their positions are also random in repeated experiments. The nonuniformities are often mesoscopic in space, such that their typical sizes are between the interaction radius and the system length. In addition, they are usually of multiscale nature, with random sizes and shapes in a dense manifold. Such nonuniformities are termed *heterogeneous*.

It is possible to show [78] that there exists a mapping between the states of an atomic cloud, subject to an alternating modulation, and the states of an atomic system in a random spatial external potential. This analogy allows for the estimation of typical parameters characterizing the process of nonequilibrium generation. Assume that such a matter has been created. How would it be possible to develop a statistical description of this matter?

Let us consider a snapshot of a heterogeneous matter consisting of the regions of two types, whose typical properties can be characterized by some quantities playing the role of local order parameters or order indices [79]. For instance, the role of the order parameters can be played by densities or some local atomic configurations. Such regions, with different order parameters, are analogous to local thermodynamic phases [80,81].

The spatial separation of the nonuniformities in a system can be described by employing the Gibbs theory of quasi-equilibrium systems [80,81]. The total system volume can be treated as a union

$$\mathbb{V} = \mathbb{V}_1 \bigcup \mathbb{V}_2 \qquad (31)$$

of two parts corresponding to two different spatial regions separated by an equimolecular surface. The convenience of using the equimolecular surface is that it allows for the additive representation of observable quantities. For instance, the system volume

and the number of particles are written as the sums

$$V = V_1 + V_2, \qquad N = N_1 + N_2. \tag{32}$$

Each subvolume is mathematically characterized by the manifold indicator function

$$\xi_\nu(\mathbf{r}) = \begin{cases} 1, & \mathbf{r} \in \mathbb{V}_\nu \\ 0, & \mathbf{r} \notin \mathbb{V}_\nu \end{cases}, \tag{33}$$

where $\nu = 1, 2$ enumerates the local phases, that is, the regions with different properties.

The quasi-equilibrium ensemble, characterizing the system, under a given spatial distribution of different regions, is the pair $\{\mathcal{H}, \hat{\rho}(\xi)\}$ of the space of microstates and a statistical operator. The space of microstates is the fiber space

$$\mathcal{H} \equiv \mathcal{H}_1 \bigotimes \mathcal{H}_2 \tag{34}$$

of weighted Hilbert spaces corresponding to the states typical of a given region (phase). The statistical operator is normalized, so that

$$\mathrm{Tr} \int \hat{\rho}(\xi)\, \mathcal{D}\xi = 1, \tag{35}$$

where the trace is taken over the Hamiltonian degrees of freedom and the functional integration is over the manifold indicator functions [4]. This functional integration characterizes the random distribution of the shapes, sizes, and locations of different regions.

To correctly define the statistical operator, one has to consider a representative statistical ensemble taking into account all constraints uniquely describing the system. In addition to the normalization condition, the standard constraint is the definition of the internal energy

$$E = \mathrm{Tr} \int \hat{\rho}(\xi)\hat{H}(\xi)\, \mathcal{D}\xi \tag{36}$$

as the average of the energy operator $\hat{H}(\xi)$. Other constraints can be represented as the statistical averages

$$C_i = \mathrm{Tr} \int \hat{\rho}(\xi)\hat{C}_i(\xi)\, \mathcal{D}\xi \tag{37}$$

of the given constraint operators $\hat{C}_i(\xi)$. The statistical operator is defined as a minimizer of the information functional

$$I[\hat{\rho}(\xi)] = \mathrm{Tr} \int \hat{\rho}(\xi)\ln\hat{\rho}(\xi)\mathcal{D}\xi + \lambda_0 \left[\mathrm{Tr} \int \hat{\rho}(\xi)\mathcal{D}\xi - 1 \right] +$$

$$+\beta \left[\mathrm{Tr} \int \hat{\rho}(\xi)\hat{H}(\xi)\mathcal{D}\xi - E \right] + \sum_i \lambda_i \left[\mathrm{Tr} \int \hat{\rho}(\xi)\hat{C}_i(\xi)\mathcal{D}\xi - C_i \right], \tag{38}$$

in which the first term is the Shannon information and λ_0, β, and λ_i are the Lagrange multipliers guaranteeing the validity of the imposed constraints. This principle of minimal information yields the statistical operator

$$\hat{\rho}(\xi) = \frac{1}{Z}\exp\{-\beta H(\xi)\}, \tag{39}$$

with the grand Hamiltonian

$$H(\xi) = \hat{H}(\xi) - \sum_i \mu_i \hat{C}_i(\xi), \tag{40}$$

where $\mu_i = -\lambda_i T$ and $T = 1/\beta$ is effective temperature. The inverse normalization factor

$$Z = \mathrm{Tr}\int \exp\{-\beta H(\xi)\}\mathcal{D}\xi$$

is the partition function.

The important point is the introduction of the effective Hamiltonian $\widetilde{H}$ by the equality

$$\int \exp\{-\beta H(\xi)\}\mathcal{D}\xi = \exp(-\beta\widetilde{H}). \tag{41}$$

Then the partition function takes the simple form

$$Z = \mathrm{Tr}e^{-\beta\widetilde{H}}, \tag{42}$$

containing only the trace over the Hamiltonian degrees of freedom. The effective temperature T, generally, can include the standard thermal noise and the energy injected into the system, as is explained in the Introduction.

The geometric weights

$$w_\nu = \int \xi_\nu(\mathbf{r})\mathcal{D}\xi \tag{43}$$

define the probabilities of the related phases, by construction, satisfying the normalization condition

$$w_1 + w_2 = 1 \qquad (0 \le w_\nu \le 1). \tag{44}$$

These probabilities are found from the minimization of the grand potential

$$\Omega = -T\ln\mathrm{Tr}e^{-\beta\widetilde{H}}. \tag{45}$$

The techniques of functional integration over the manifold indicator functions are thoroughly explained in Ref. [4]. Below, we shall employ these techniques omitting, for brevity, intermediate calculations.

5. STATISTICAL MODEL OF GRAIN TURBULENCE

As has been mentioned above, the regime of grain turbulence is one of the most difficult for theoretical description, if one wishes to consider the details of its nonequilibrium and nonuniform spatio-temporal behavior. However, if one is interested in its average statistical properties, it is possible to invoke the approach of the previous section. This is admissible, since the local-equilibrium time t_{loc} is much shorter than the lifetime of this regime t_{het}. Here we advance a statistical model that can grasp the main average features of the heterophase granular state.

The granular state can be treated as a heterophase mixture of Bose-condensed grains immersed into the cloud consisting of normal (non-condensed) atoms. Starting with the local-equilibrium Gibbs ensemble [80,81], we average over all random heterogeneous configurations, as is sketched above, with the related mathematics thoroughly expounded in reviews [4,5,82]. The resulting effective Hamiltonian of the mixture becomes the sum of two Hamiltonian replicas

$$\widetilde{H} = H_1 \bigoplus H_2. \tag{46}$$

The Hamiltonian is defined on the fiber space (34). The term H_1 acts on the space of microstates $\mathcal{H}_1$ with broken global gauge symmetry $U(1)$, corresponding to the Bose-condensed phase [83], while the term H_2, on the space of microstates $\mathcal{H}_2$ with preserved gauge symmetry.

The Bose-condensed phase is characterized by a representative ensemble [84-87], with the grand Hamiltonian

$$H_1 = \hat{H}_1 - \mu_0 N_0 - \mu_1 \hat{N}_1 - \hat{\Lambda}. \tag{47}$$

Here the energy operator is

$$\hat{H}_1 = w_1 \int \hat{\psi}^\dagger(\mathbf{r}) \left[-\frac{\nabla^2}{2m} + U(\mathbf{r}) \right] \hat{\psi}(\mathbf{r}) d\mathbf{r} +$$

$$+ \frac{w_1^2}{2} \int \hat{\psi}^\dagger(\mathbf{r}) \hat{\psi}^\dagger(\mathbf{r}') \Phi(\mathbf{r} - \mathbf{r}') \hat{\psi}(\mathbf{r}') \hat{\psi}(\mathbf{r}) \, d\mathbf{r} d\mathbf{r}', \tag{48}$$

in which $U(\mathbf{r})$ is an external potential, $\Phi(\mathbf{r})$ is the interaction potential, and the Bose field operators are shifted, according to Bogoliubov [88,89], thus, breaking the gauge symmetry,

$$\hat{\psi}(\mathbf{r}) = \eta(\mathbf{r}) + \psi_1(\mathbf{r}). \tag{49}$$

In this shift, $\eta(\mathbf{r})$ is the condensate wave function and $\psi_1(\mathbf{r})$ is the field operator of uncondensed atoms, these terms being orthogonal to each other,

$$\int \eta^*(\mathbf{r}) \psi_1(\mathbf{r}) \, d\mathbf{r} = 0, \tag{50}$$

which excludes the double counting. The Lagrange multipliers μ_0 and μ_1 guarantee the validity of the normalization conditions for the number of condensed atoms

$$N_0 = w_1 \int |\eta(\mathbf{r})|^2 d\mathbf{r} \tag{51}$$

and for that of uncondensed atoms

$$N_1 = w_1 \int \langle \psi_1^\dagger(\mathbf{r})\psi_1(\mathbf{r}) \rangle d\mathbf{r}. \tag{52}$$

The last operator $\hat{\Lambda}$ in Eq. (47) is the Lagrange term preserving the condition

$$\langle \psi_1(\mathbf{r}) \rangle = 0 \tag{53}$$

defining the condensate wave function as an order parameter

$$\eta(\mathbf{r}) = \langle \hat{\psi}(\mathbf{r}) \rangle. \tag{54}$$

The grand Hamiltonian of the normal (gauge-symmetric) phase is

$$H_2 = \hat{H}_2 - \mu_2 \hat{N}_2. \tag{55}$$

Here the energy operator is

$$\hat{H}_2 = w_2 \int \psi_2^\dagger(\mathbf{r}) \left[-\frac{\nabla^2}{2m} + U(\mathbf{r}) \right] \psi_2(\mathbf{r}) d\mathbf{r} +$$

$$+ \frac{w_2^2}{2} \int \psi_2^\dagger(\mathbf{r})\psi_2^\dagger(\mathbf{r}')\Phi(\mathbf{r}-\mathbf{r}')\psi_2(\mathbf{r}')\psi_2(\mathbf{r}) \, d\mathbf{r}d\mathbf{r}'. \tag{56}$$

The Lagrange multiplier μ_2 guarantees the validity of the normalization for the number of atoms in the normal phase,

$$N_2 = w_2 \int \langle \psi_2^\dagger(\mathbf{r})\psi_2(\mathbf{r}) \rangle d\mathbf{r}. \tag{57}$$

The total number of atoms in the system is

$$N = N_0 + N_1 + N_2. \tag{58}$$

The corresponding atomic fractions

$$n_0 \equiv \frac{N_0}{N}, \qquad n_1 \equiv \frac{N_1}{N}, \qquad n_2 \equiv \frac{N_2}{N} \tag{59}$$

satisfy the normalization

$$n_0 + n_1 + n_2 = 1. \tag{60}$$

The condition of heterophase quasi-equilibrium [4,5,82] leads to the relation

$$\mu_0 n_0 + \mu_1 n_1 = (n_0 + n_1)\mu_2 \tag{61}$$

between the Lagrange multipliers.

The geometric weights of the phases are defined as the minimizers of the grand potential. This, with the notation

$$w_1 \equiv w, \qquad w_2 \equiv 1 - w, \tag{62}$$

implies the conditions

$$\frac{\partial \Omega}{\partial w} = 0, \qquad \frac{\partial^2 \Omega}{\partial w^2} > 0. \tag{63}$$

The first of Eqs. (63), with the use of the notations

$$K_1 \equiv \int \langle \hat{\psi}(\mathbf{r}) \left[-\frac{\nabla^2}{2m} + U(\mathbf{r}) \right] \hat{\psi}(\mathbf{r}) \rangle d\mathbf{r} - \mu_0 \int |\eta(\mathbf{r})|^2 d\mathbf{r} - \mu_1 \int \langle \psi_1^\dagger(\mathbf{r}) \psi_1(\mathbf{r}) \rangle d\mathbf{r},$$

$$K_2 \equiv \int \langle \psi_2^\dagger(\mathbf{r}) \left[-\frac{\nabla^2}{2m} + U(\mathbf{r}) \right] \psi_2(\mathbf{r}) \rangle d\mathbf{r} - \mu_2 \int \langle \psi_2^\dagger(\mathbf{r}) \psi_2(\mathbf{r}) \rangle d\mathbf{r},$$

$$\Phi_1 \equiv \int \langle \hat{\psi}^\dagger(\mathbf{r}) \hat{\psi}^\dagger(\mathbf{r}') \Phi(\mathbf{r} - \mathbf{r}') \hat{\psi}(\mathbf{r}') \hat{\psi}(\mathbf{r}) \rangle d\mathbf{r} d\mathbf{r}',$$

$$\Phi_2 \equiv \int \langle \psi_2^\dagger(\mathbf{r}) \psi_2^\dagger(\mathbf{r}') \Phi(\mathbf{r} - \mathbf{r}') \psi_2(\mathbf{r}') \psi_2(\mathbf{r}) \rangle d\mathbf{r} d\mathbf{r}',$$

yields the equation

$$w = \frac{\Phi_2 + K_2 - K_1}{\Phi_1 + \Phi_2} \tag{64}$$

for the weight of the Bose-condensed phase.

The second of Eqs. (63) is the stability requirement imposing the necessary condition

$$\Phi_1 + \Phi_2 > 0. \tag{65}$$

This tells us that the effective atomic interactions must be repulsive in order that the heterophase granular mixture would be stable.

It is worth emphasizing the necessity of nonzero atomic interactions for the Bose-condensed system to be stable. The ideal Bose gas is a pathological object that cannot form a stable Bose-Einstein condensate because of thermodynamically anomalous particle fluctuations and diverging compressibility [12,18,19,77,90,91], although non-condensed ideal Bose gas can be stable [92]. But in the ideal Bose gas, there can be neither vortices, nor vortex turbulence, nor grain turbulence, whose existence is due to the nonlinearity caused by atomic interactions.

6. MESOSCOPIC MIXTURE OF TWO PHASES

Dealing with the above expressions describing a mesoscopic mixture is a rather involved problem requiring the use of nontrivial approximations. Meanwhile, in order to illustrate how the above approach works, we consider a simplified model that

can exhibit the mesoscopic coexistence of two phases, one with broken gauge symmetry and another with the conserved gauge symmetry. The choice of this model is done keeping in mind that Bose-Einstein condensation is necessarily accompanied by the global gauge symmetry breaking [83], while the normal, non-condensed phase conserves this symmetry. The other advantage of the chosen model is its simplicity allowing for a straightforward demonstration of the applicability of the suggested approach. The phase with conserved gauge symmetry is called disordered and that with the broken symmetry, ordered. The regions of the ordered phase, surrounded by the disordered phase, are mesoscopic in the sense that their average sizes are larger than the interaction radius, but much shorter than the system linear size. This model can be considered as a cartoon of a system consisting of Bose-condensed droplets surrounded by normal uncondensed gas.
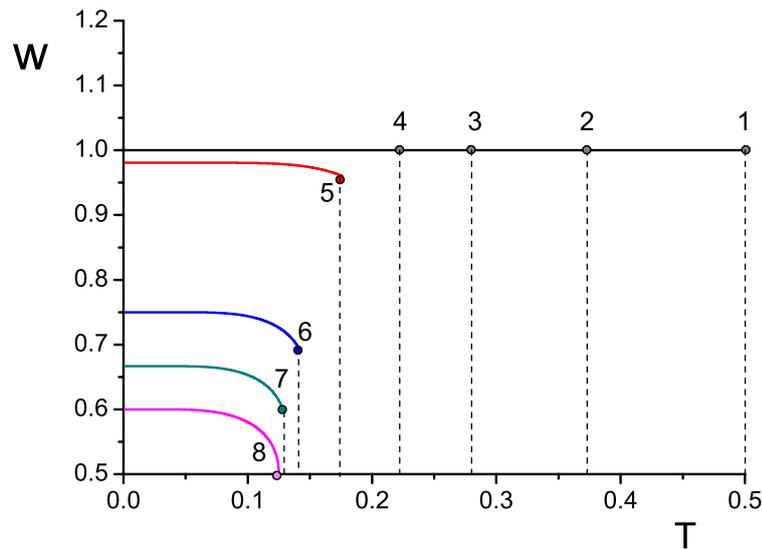

Fig. 1 – Probability of the ordered phase as a function of the dimensionless effective temperature for different parameters u: (1) $u = 0$; (2) $u = 0.1$; (3) $u = 0.3$; (4) $u = 0.4$; (5) $u = 0.51$; (6) $u = 0.75$; (7) $u = 1$; (8) $u = 1.5$. The dots mark the points of the transition from the broken-symmetry phase with a nonzero order parameter to the gauge-symmetric phase with zero order parameter.

One should not confuse the considered system with mesoscopic thermal disorder with a system in a random potential that induces microscopic quenched disorder [93]. The latter system can be equilibrium, while the former is only quasi-equilibrium.
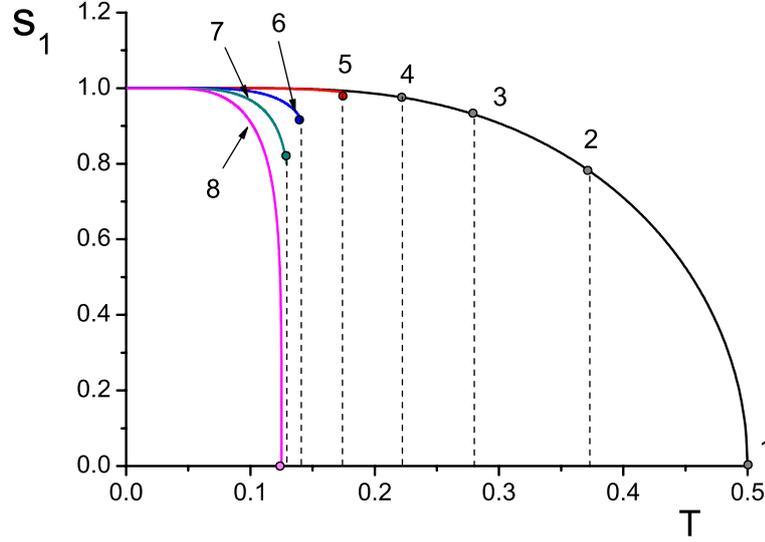
Fig. 2 – Order parameter as a function of the dimensionless effective temperature for different parameters u: (1) $u = 0$; (2) $u = 0.1$; (3) $u = 0.3$; (4) $u = 0.4$; (5) $u = 0.51$; (6) $u = 0.75$; (7) $u = 1$; (8) $u = 1.5$. The dots mark the points of the transition from the broken-symmetry phase with a nonzero order parameter to the gauge-symmetric phase with zero order parameter.

Let us consider an insulating optical lattice, where atoms can occupy several energy levels E_n. Atoms are assumed to interact through long-range forces, such as spinor or dipole forces [94]. We start with the standard Hamiltonian in term of the field operators $\psi(\mathbf{r})$ that can be expanded over atomic orbitals,

$$\psi(\mathbf{r}) = \sum_{nj} c_{nj} \varphi_{nj}(\mathbf{r}), \tag{66}$$

where the index n labels energy levels E_n and j enumerates lattice cites. Keeping in mind unity filling factor, we impose the no-double-occupancy condition

$$\sum_n c_{nj}^\dagger c_{nj} = 1, \qquad c_{mj} c_{nj} = 0. \tag{67}$$

Taking account of only two lowest energy levels makes it possible to introduce the pseudospin operators S_j^α by means of the transformation

$$c_{1j}^\dagger c_{1j} = \frac{1}{2} + S_j^x, \qquad c_{2j}^\dagger c_{2j} = \frac{1}{2} - S_j^x,$$

$$c_{1j}^\dagger c_{2j} = S_j^z - iS_j^y, \qquad c_{2j}^\dagger c_{1j} = S_j^z + iS_j^y. \tag{68}$$

Assume that the system consists of the random mixture of two different phases. One phase has broken gauge symmetry and the other is gauge symmetric. By accomplishing the averaging over the manifold indicator functions [4], we come to the effective Hamiltonian

$$\widetilde{H} = H_1 \bigoplus H_2,$$

$$H_\nu = w_\nu N E_0 + \frac{w_\nu^2}{2} \sum_{i \neq j} A_{ij} - w_\nu \Omega_0 \sum_j S_j^x + w_\nu^2 \sum_{i \neq j} \left(B_{ij} S_i^x S_j^x - I_{ij} S_i^z S_j^z \right), \quad (69)$$

in which A_{ij}, B_{ij}, I_{ij} are the matrix elements of the atomic interaction potential [95] and

$$E_0 \equiv \frac{1}{2}(E_1 + E_2), \qquad \Omega_0 \equiv E_2 - E_1. \tag{70}$$

This Hamiltonian is invariant under the gauge transformation

$$S_j^z \longrightarrow e^{i\alpha} S_j^z, \tag{71}$$

in which α is a real number. The pseudospin average, depending on the considered phase, can be calculated in two ways,

$$\langle S_j^z \rangle_\nu \equiv \mathrm{Tr}_{\mathcal{H}_\nu} \hat{\rho}_\nu S_j^z \qquad (\nu = 1, 2), \tag{72}$$

with different statistical operators

$$\hat{\rho}_\nu \equiv \frac{\exp(-\beta H_\nu)}{\mathrm{Tr}_{\mathcal{H}_\nu} \exp(-\beta H_\nu)} \tag{73}$$

and over different spaces of microscopic states typical of the given phase. The phase with broken gauge symmetry corresponds to the nonzero average

$$\langle S_j^z \rangle_1 \neq 0, \tag{74}$$

while the phase with the conserved symmetry gives

$$\langle S_j^z \rangle_2 = 0. \tag{75}$$

The order parameters are defined as

$$s_\nu \equiv \frac{2}{N} \sum_{j=1}^{N} \langle S_j^z \rangle_\nu. \tag{76}$$

For the phases with the broken symmetry and unbroken symmetry, one has, respectively,

$$s_1 \neq 0, \qquad s_2 = 0. \tag{77}$$

To calculate the order parameter s_1 and the phase probabilities w_ν, we resort to the mean-field approximation, with the use of the notations

$$u \equiv \frac{A}{I+B}, \qquad b \equiv \frac{B}{I+B}, \qquad \omega \equiv \frac{\Omega_0}{I+B},$$

$$A \equiv \frac{1}{N} \sum_{i \neq j}^{N} A_{ij}, \qquad B \equiv \frac{1}{N} \sum_{i \neq j}^{N} B_{ij}, \qquad I \equiv \frac{1}{N} \sum_{i \neq j}^{N} I_{ij}. \tag{78}$$

Then, the minimization of the grand potential Ω yields the equations

$$w_1 = \frac{2u + \omega_1 x_1 - \omega_2 x_2}{4u - (1-b)s_1^2}, \qquad w_2 = 1 - w_1,$$

$$\sqrt{(w_1 s_1)^2 + \omega^2} = w_1 \tanh\left[\frac{(1-b)w_1}{2T} \sqrt{(w_1 s_1)^2 + \omega^2} \right], \tag{79}$$

in which the effective temperature T is measured in units of $I+B$ and

$$\omega_1 = (1-b)\omega, \qquad \omega_2 = \omega - bw_2 x_2,$$

$$x_1 = \frac{\omega}{w_1}, \qquad x_2 = \tanh\left(\frac{w_2 \omega_2}{2T} \right). \tag{80}$$

We solved these equations numerically for $b \ll 1$, $\omega \ll 1$, and for varying u. At $T = 0$, the order parameter $s_1 = 1$. It monotonically decreases with rising T up to a phase-transition point, where s_1 becomes zero and the system transfers to a disordered phase with unbroken gauge symmetry. The phase transition is of second order for $u \leq 0$ and $u \geq 3/2$, while of first order for $0 < u < 3/2$. The behavior of w_1 and s_1 as functions of T is shown in Figs. 1 and 2. This model illustrates that, for some system parameters and for sufficiently high effective temperature that includes the injected energy, the system, can, first, become a mixture of two phases, one with broken gauge symmetry and the other with unbroken symmetry, and at a large effective temperature T the whole system transfers to the disordered phase with unbroken symmetry, that is, becomes normal gauge-symmetric phase.

7. CONCLUSION

The idea is advanced that strong perturbations of an initially equilibrium Bose-condensed gas lead to the sequence of nonequilibrium states whose order is inverse to the sequence of states arising in the process of the Bose-gas relaxation from an initial nonequilibrium non-condensed state to its equilibrium Bose-condensed state.

We have described a general approach for constructing statistical models of nonequilibrium Bose gases. The method is based on the averaging over heterogenous configurations of a nonequilibrium system.

A statistical model of grain turbulence is suggested, whose general properties are formulated. Numerical calculations for a simple model, in the frame of a mean-field approximation, show that the grain turbulence can exist in a region of injected energies. Increasing the amount of energy, injected into the system above the threshold, leads to the destruction of the regime of grain turbulence, so that the system passes to a normal non-condensed state with the preserved gauge symmetry. The gauge-symmetric phase represents the wave turbulence of normal, non-condensed gas. The transformation of the gauge-broken phase into the gauge-symmetric phase plays the role of the transition from the grain turbulence to wave turbulence.

REFERENCES

1. C. K. Tam and K. C. Chen, J. Fluid Mech. **92**, 303 (1979).
2. R. H. Kraichnan and D. Montgomery, Rep. Prog. Phys. **43**, 547 (1980).
3. V. I. Yukalov, Laser Phys. Lett. **7**, 467 (2010).
4. V. I. Yukalov, Phys. Rep. **208**, 395 (1991).
5. V. I. Yukalov, Int. J. Mod. Phys. **17**, 2333 (2003).
6. V. I. Yukalov, E. P. Yukalova, and V. S. Bagnato, Laser Phys. **12**, 231 (2002).
7. E. H. Lieb, R. Seiringer, J. P. Solovej, and J. Yngvason, *The Mathematics of the Bose Gas and Its Condensation* (Birkhauser, Basel, 2005).
8. V. Letokhov, *Laser Control of Atoms and Molecules* (Oxford University Press, New York, 2007).
9. C. J. Pethick and H. Smith, *Bose-Einstein Condensation in Dilute Gases* (Cambridge University Press, Cambridge, 2008).
10. P. W. Courteille, V. S. Bagnato, and V. I. Yukalov, Laser Phys. **11**, 659 (2001).
11. J. O. Andersen, Rev. Mod. Phys. **76**, 599 (2004).
12. V. I. Yukalov, Laser Phys. Lett. **1**, 435 (2004).
13. K. Bongs and K. Sengstock, Rep. Prog. Phys. **67**, 907 (2004).
14. V. I. Yukalov and M. D. Girardeau, Laser Phys. Lett. **2**, 375 (2005).
15. A. Posazhennikova, Rev. Mod. Phys. **78**, 1111 (2006).
16. N. P. Proukakis and B. Jackson, J. Phys. B **41**, 203002 (2008).
17. V. A. Yurovsky, M. Olshanii, and D. S. Weiss, Adv. At. Mol. Opt. Phys. **55**, 61 (2008).
18. V. I. Yukalov, Laser Phys. **19**, 1 (2009).
19. V. I. Yukalov, Phys. Part. Nucl. **42**, 460 (2011).
20. V. I. Yukalov, E. P. Yukalova, and V. S. Bagnato, Phys. Rev. A **56**, 4845 (1997).
21. J. A. Seman, E. A. L. Henn, M. Haque, R. F. Shiozaki, E. R. F. Ramos, M. Caracanhas, P. Castilho, C. Castelo Branco, P. E. S. Tavares, F. J. Poveda-Cuevas, G. Roati, K. M. F. Magalhães, and V. S. Bagnato, Phys. Rev. A **82**, 033616 (2010).
22. V. I. Yukalov, E.P. Yukalova, and V. S. Bagnato, Phys. Rev. A **66**, 043602 (2002).
23. V. I. Yukalov, Acta Phys. Pol. A **57**, 295 (1980).
24. Z. Dutton, M. Budde, C. Slowe, and L. V. Hau, Science **293**, 663 (2001).

25. V. I. Yukalov and E. P. Yukalova, Laser Phys. Lett. **1**, 50 (2004).

26. J. Ruostekoski and Z. Dutton, Phys. Rev. A **72**, 063626 (2005).

27. I. Shomroni, E. Lahoud, S. Levy, and J. Steinhauer, Nature Phys. **5**, 193 (2009).

28. M. Ma, R. Carretero-Gonzalez, P. G. Kevrekidis, D. J. Frantzeskakis, and B. A. Malomed, Phys. Rev. A **82**, 023621 (2010).

29. S. Ishiro, M. Tsubota, and H. Takeuchi, Phys. Rev. A **83**, 063602 (2011).

30. T. P. Simula, Phys. Rev. A **84**, 021603 (2011).

31. E. A. L. Henn, J. A. Seman, G. Roati, K. M. F. Magalhães, and V. S. Bagnato, Phys. Rev. Lett. **103**, 045301 (2009).

32. J. A. Seman, R. F. Shiozaki, F. J. Poveda-Cuevas, E. A. L. Henn, K. M. F. Magalhães, G. Roati, G. D. Telles, and V. S. Bagnato, J. Phys. Conf. Ser. **264**, 012004 (2011).

33. R. F. Shiozaki, G. D. Telles, V. I. Yukalov, and V. S. Bagnato, Laser Phys. Lett. **8**, 393 (2011).

34. J. A. Seman, E. A. L. Henn, R. F. Shiozaki, G. Roati, F. J. Poveda-Cuevas, K. M. F. Magalhães, V. I. Yukalov, M. Tsubota, M. Kobayashi, K. Kasamatsu, and V. S. Bagnato, Laser Phys. Lett. **8**, 691 (2011).

35. V. S. Bagnato and V. I. Yukalov, Prog. Opt. Sci. Photon. **1**, 377 (2013).

36. J. A. Seman, E. A. L. Henn, M. Haque, R. F. Shiozaki, E. R. F. Ramos, M. Caracanhas, P. Castilho, C. Castelo Branco, P. E. S. Tavares, F. J. Poveda-Cuevas, G. Roati, K. M. F. Magalhães, and V. S. Bagnato, Phys. Rev. A **82**, 033616 (2010).

37. E. A. L. Henn, J. A. Seman, E. R. F. Ramos, M. Caracanhas, P. Castilho, E. P. Olimpio, G. Roati, D. V. Magalhães, K. M. F. Magalhães, and V. S. Bagnato, Phys. Rev. A **79**, 043618 (2009).

38. E. R. F. Ramos, E. A. L. Henn, J. A. Seman, M. A. Caracanhas, K. M. F. Magalhães, K. Helmerson, V. I. Yukalov, and V. S. Bagnato, Phys. Rev. A **78**, 063412 (2008).

39. S. E. Pollack, D. Dries, R. G. Hulet, K. M. F. Magalhães, E. A. L. Henn, E. R. F. Ramos, M. A. Caracanhas, and V. S. Bagnato, Phys. Rev. A **81**, 053627 (2010).

40. S. E. Pollack, D. Dries, M. Junker, Y. P. Chen, T. A. Corcovilos, and R. G. Hulet, Phys. Rev. Lett. **102**, 090402 (2009).

41. S. E. Pollack, D. Dries, and R. G. Hulet, Science **326**, 1683 (2009).

42. E. Timmermans, P. Tommasini, M. Hussein, and A. Kerman, Phys. Rep. **315**, 199 (1999).

43. E. Levich and V. Yakhot, Phys. Rev. B **15**, 243 (1977).

44. H. T. C. Stoof, Phys. Rev. A **45**, 8398 (1992).

45. H. T. C. Stoof, Phys. Rev. Lett. **78**, 768 (1997).

46. D. W. Snoke and J. P. Wolfe, Phys. Rev. B **39**, 4030 (1989).

47. D. V. Semikoz and I. I. Tkachev, Phys. Rev. D **55**, 489 (1997).

48. K. Damle, S. N. Majumdar, an S. Sachdev, Phys. Rev. A **54**, 5037 (1996).

49. P. D. Drummond and J. F. Corney, Phys. Rev. A **60**, 2661 (1999).

50. Y. Kagan and B. V. Svistunov, J. Exp. Theor. Phys. **78**, 187 (1994).

51. Y. Kagan and B. V. Svistunov, Phys. Rev. Lett. **79**, 3331 (1997).

52. N. G. Berloff and B. V. Svistunov, Phys. Rev. A **66**, 013603 (2002).

53. J. Sopik, C. Sire, and P. H. Chavanis, Phys. Rev. E **74**, 011112 (2006).

54. B. Svistunov, Phys. Lett. A **287**, 169 (2001).

55. C. W. Gardiner, P. Zoller, R. J. Ballagh, and M. J. Davis, Phys. Rev. Lett. **79**, 1793 (1997).

56. C. W. Gardiner, M. D. Lee, R. J. Ballagh, M. J. Davis, and P. Zoller, Phys. Rev. Lett. **81**, 5266 (1998).

57. M. Köhl, M. J. Davis, C. W. Gardiner, T. W. Hänsch, and T. Esslinger, Phys. Rev. Lett. **88**, 080402 (2002).

58. V. E. Zakharov and S. V. Nazarenko, Physica D **201**, 203 (2005).
59. M. Hugbart, J. A. Retter, A. F. Varon, P. Bouyer, A. Aspect, and M. J. Davis, Phys. Rev. A **75**, 011602 (2007).
60. S. Ritter, A. Öttl, T. Donner, T. Bourdel, M. Köhl, and T. Esslinger, Phys. Rev. Lett. **98**, 090402 (2007).
61. M. C. Garrett, A. Ratnapala, E. D. van Ooijen, C. J. Vale, K. Weegink, S. K. Schnelle, O. Vainio, N. R. Heckenberg, H. Rubinsztein-Dunlop, and M. J. Davis, Phys. Rev. A **83**, 013630 (2011).
62. R. P. Smith, S. Beattie, S. Moulder, R. L. D. Campbell, and Z. Hadzibabic, Phys. Rev. Lett. **109**, 105301 (2012).
63. A. J. Allen, N. G. Parker, N. P. Proukakis, and C. F. Barenghi, arXiv:1401.7257 (2014).
64. M. Tsubota, K. Kasamatsu, and M. Kobayashi, arXiv:1004.5458 (2010).
65. M. Tsubota, M. Kobayashi, and H. Takeushi, Phys. Rep. **522**, 191 (2013).
66. K. E. Wilson, E. C. Samson, Z. L. Newman, T. W. Neely, and B. P. Anderson, Ann. Rev. Cold At. Mol. **1**, 261 (2013).
67. S. K. Nemirovskii, Phys. Rep. **524**, 85 (2013).
68. T. W. B. Kibble, J. Phys. A **9**, 1387 (1976).
69. W. H. Zurek, Nature **317**, 505 (1985).
70. W. H. Zurek, Phys. Rep. **276**, 177 (1996).
71. C. N. Weiler, T. W Neely, D. R. Scherer, A. S. Bradley, M. J. Davis, and B. P. Anderson, Nature **455**, 948 (2008).
72. S. Khlebnikov and I. Tkachev, Phys. Rev. D **61**, 083517 (2000).
73. N. N. Bogoliubov, J. Exp. Theor. Phys. **18**, 622 (1948).
74. N. N. Bogoliubov, *On the Problem of Hydrodynamics of Superfluid Liquid* (JINR, Dubna, 1963).
75. S. V. Iordansky, Dokl. Phys. **153**, 74 (1963).
76. V. I. Yukalov, Laser Phys. Lett. **8**, 485 (2011).
77. J. L. Birman, R. G. Nazmitdinov, and V. I. Yukalov, Phys. Rep. **526**, 1 (2013).
78. V. I. Yukalov, E. P. Yukalova, and V. S. Bagnato, Laser Phys. **19**, 686 (2009).
79. A. J. Coleman and V. I. Yukalov, *Reduced Density Matrices* (Springer, Berlin, 2000).
80. J. W. Gibbs, Collected Works, Vol. 1 (Longmans, New York, 1928).
81. J. W. Gibbs, Collected Works, Vol. 2 (Longmans, New York, 1931).
82. V. I. Yukalov, Symmetry **2**, 40 (2010).
83. V. I. Yukalov, Laser Phys. Lett. **4**, 632 (2007).
84. V. I. Yukalov, Phys. Lett. A **359**, 712 (2006).
85. V. I. Yukalov and E.P. Yukalova, Phys. Rev. A **74**, 063623 (2006).
86. V. I. Yukalov and E.P. Yukalova, Phys. Rev. A **76**, 013602 (2007).
87. V. I. Yukalov, Ann. Phys. **323**, 461 (2008).
88. N. N. Bogoliubov, *Lectures on Quantum Statistics*, Vol. 1 (Gordon and Breach, New York, 1967).
89. N. N. Bogoliubov, *Lectures on Quantum Statistics*, Vol. 2 (Gordon and Breach, New York, 1970).
90. V. I. Yukalov, Phys. Rev. E **72**, 066119 (2005).
91. J. Bosse, K. N. Pathak, and G. S. Singh, Phys. Rev. E **84**, 042101 (2011).
92. J. Esteve, J. B. Trebbia, T. Schumm, A. Aspect, C. I. Westbrook, and I. Bouchoule, Phys. Rev. Lett. **96**, 130403 (2006).
93. V. I. Yukalov and R. Graham, Phys. Rev. A **75**, 023619 (2007).
94. Y. Kawaguchi and M. Ueda, Phys. Rep. **520**, 253 (2012).
95. V. I. Yukalov and E. P. Yukalova, Laser Phys. **21**, 1448 (2011).